Three-body interactions in complex fluids: virial coefficients from simulation finite-size effects

Douglas J. Ashton[1] and Nigel B. Wilding[1]

[1]*Department of Physics, University of Bath, Bath BA2 7AY, United Kingdom*

A simulation technique is described for quantifying the contribution of three-body interactions to the thermodynamical properties of coarse-grained representations of complex fluids. The method is based on a new approach for determining virial coefficients from the measured volume-dependent asymptote of a certain structural function. By comparing the third virial coefficient B_3 for a complex fluid with that of an approximate coarse-grained model described by a pair potential, three body effects can we quantified. The strategy is applicable to both Molecular Dynamics and Monte Carlo simulation. Its utility is illustrated via measurements of three-body effects in models of star polymers and in highly size-asymmetrical colloid-polymer mixtures.

I. INTRODUCTION

The task of determining the thermodynamical properties of complex fluids by analytical or computational means is often complicated by a profusion of degrees of freedom on small length scales. For instance, in order to simulate a system of large flexible molecules such as polymers or biomolecules, considerable computational effort must be invested to deal with the vibrational motion of the individual atoms. Since such motion typically occurs on much shorter timescales than the relaxation of the system as a whole, this causes difficulty in probing thermodynamical behaviour. Similarly for systems such as colloidal dispersions, in which large colloid particles are immersed in a sea of much smaller particles, the relaxation of the large particles is typically extremely slow. This is because the small particles hem in the large ones, hindering their motion.

To tackle such problems "coarse-graining" strategies have been developed. These seek to integrate out the degrees of freedom on short length scales, leaving a simpler system in which the surviving coordinates are assumed to interact via effective interactions. In principle if the integration is performed exactly, the effective interactions will account exactly for the effects of the degrees of freedom which have been subsumed. Accordingly, the statistical properties of the surviving coordinates will be identical in both the coarse-grained and the full model. Often, however, the task of performing an exact coarse-graining is extremely challenging, chiefly because the effective potential is many-body in character even when the underlying interactions are pairwise additive. It is therefore common practice to implement an approximate coarse-graining in which the full many-body effective potential is replaced by a simpler one involving only pair interactions. Such an approximation is widely used in theories and simulations of complex fluids because the pair potential itself is usually straightforward to obtain, either analytically or from a simulation of two molecules. Once it is obtained one can use it to study the properties of a many particle system[1–3].

Two examples of systems to which coarse-graining is frequently applied are displayed in Fig. 1. In the first, a system of star polymers, each molecule is replaced by a single soft effective particle centred on the core atom. These particles interact via a soft pair potential (the "potential of mean force") reflecting the fact that two star polymers can substantially overlap. In the second example, a highly size-asymmetrical binary mixture, the small spheres mediate interactions between the large ones known as "depletion" forces[4]. Formally the effective interaction between the large particles is many-body in form, but this is typically approximated in terms of a depletion pair potential.

fig1.eps

FIG. 1. (Left part) A snapshot of three star polymers. The big spheres represent a coarse grained model in which each polymer is replaced by a single effective particle described by a potential of mean force. (Right part) Snapshot of a highly size-asymmetrical mixture of spheres. The effective one-component model is realized by tracing over the small sphere degrees of freedom.

Given the prevalence of the pair potential approximation in coarse-grained representations of complex fluids, there is a need to be able to quantify its effects on the thermodynamics of model systems. In this paper, we describe a method for determining the scale of three-body interactions which will usually be the most prominent of the neglected many-body terms in the approximate coarse-grained model[5]. In common with work of D'Adamo et al[6,7], our approach is based on a comparison of the third virial coefficient B_3 of the full model with that of its pair potential representation. To obtain B_3 in both cases, we introduce a new technique which relates its value to the finite-size effects in the asymptote of a simple-to-measure structural quantity.

The organization of our paper as follows. In Sec. II we briefly review existing methods for calculating virial coefficients and discuss why they seem (as yet) unequal to the task of dealing with many complex fluids. Sec. III describes the statistical mechanical background to our method for determining low order virial coefficients. A commentary regarding optimization issues, and the wider context of the method is given in Sec. IV. Thereafter in Secs. VI and VII we apply it to quantify the contribution of three-body interactions to the third virial coefficient for two coarse-grained models of complex fluids. A summary of our findings features in Sec. VIII.

II.   ROUTES TO VIRIAL COEFFICIENTS

The virial coefficients appear in the virial expansion of the equation of state of many-particle systems and as such are key quantities in the thermodynamical description of fluids. Their utility is manifold. At a basic level they measure the deviation of the fluid properties from those of an ideal gas. More generally, they provide a framework for systematically calculating the thermodynamical properties of a fluid and relating these to the nature of the microscopic interactions, including features such as potential range[8], molecular flexibility[7,9] and many-body forces[10].

For these and other reasons, substantial activity has been devoted to calculating virial coefficients for model systems. Much of this effort has focused on prototypical fluid models such as hard and soft spheres and spheroids[11]. Almost invariably, the approach taken involves a direct assault on the cluster integrals that provide a compact mathematical representation of the virial coefficients in terms of Mayer functions[12]. We shall refer to this as the Mayer function route. For low order virials it is often possible to make analytical progress via this route for simple models. For higher order virials and molecular systems, numerical simulation is generally required[13–15]. In this latter context a particularly powerful technique is the Mayer Sampling Method (MSM)[16–18]. This is a Monte Carlo (MC) scheme which employs ideas borrowed from free energy perturbation methods to relate the virial coefficients of the system of interest to those of a reference system for which the virial coefficients are independently known. For simple systems the MSM is the method of choice and has been highly successful in calculating virial coefficients to quite high order with impressive precision.

However, when applied to complex flexible molecules such as polymers, the complexity of implementing computational strategies based on the Mayer function route seems to increase rapidly[19]. For example, to date, calculations of virial coefficients for molecules have been limited to simple united atom representations[9], while for flexible molecules such as polymers, most studies have been based on simple lattice walks[19–22], with only a few results appearing for continuum models of modest chain

length[6,23]. The difficulties seem to arise in part from the need to explicitly integrate products of Mayer functions over molecular conformations, while also calculating further terms in the cluster integral arising from the molecular flexibility[9,19]. Additionally, when implementing the MSM for 'soft' particles such as polymers there is a lack of an obvious reference system. Consequently there is a relative scarcity of simulation measurements of measurements of third virial coefficients for complex molecules.

There is one class of complex fluid for which the Mayer function route seems unable to provide estimates of virial coefficients. This is the case of a single component effective system obtained by integrating out the degrees of freedom of a second species. Examples are colloid-polymer mixtures or molecules in explicit solvent which are often modelled as a highly size-asymmetrical binary mixture. Here one typically considers an effective one component fluid of the large particles with interactions determined implicitly by the small ones in which they are immersed. These effective interactions are inherently many-body in form, and are generally not calculable by contemporary means. However, without knowledge of their form, the Mayer function route cannot estimate the virial coefficients of the effective system. Often, however, it is possible to perform simulations of small numbers of the large particles in a sea of the small ones. The ability to deduce the virial coefficients of the effective fluid from these simulations would be useful as it would allow one to predict its likely phase behaviour at higher densities of the large particles.

III.   METHOD

In view of these issues it is interesting to explore alternatives to the Mayer function route. One such alternative is well known. It is based on the derivation of the virial expansion from the grand canonical partition function[24]; we shall refer to it as the partition function route. As discussed below, this approach expresses the Nth virial coefficient, B_N, in terms of sums and differences of products of the partition function integrals $Z_1 \ldots Z_N$. Heretofore the partition function route has been largely discounted on dual grounds. Firstly, to calculate a given virial coefficient entails the calculation of multiple integrals – in contrast to the Mayer formulation which requires only a single integral. Secondly, it potentially suffers from rapidly deteriorating precision as N increases because it estimates the relatively small value of B_N as a difference of large numbers[10].

In this section we show that the need to perform explicit numerical integration of the partition functions $Z_1 \ldots Z_N$ can be circumvented by means of a simple simulation sampling procedure which directly determines relevant ratios of these integrals via measurements of the volume-dependent asymptotic value, $f(V)$, of a *structural* function $g'_N(r_{\min})$. This function depends solely on relative molecular position, and as such is as easy to mea-

sure for complex molecules as it is for point particles. By the same token, it is obtainable by any simulation scheme capable of generating equilibrium configurations, such as Molecular Dynamics, Monte Carlo or Langevin Dynamics. Furthermore, since virial coefficients are derived from structural information rather than integration of Boltzmann factors, no knowledge of the effective interaction potential is required. This permits deployment of the method to subsets of particles, as is relevant for coarse-grained models such as effective fluids, as discussed above.

A. Low order virial coefficients of molecular systems

Consider a simulation box of volume V containing a small fixed number N of interacting molecules in thermal equilibrium at inverse temperature $\beta = (k_B T)^{-1}$. Let each molecule be comprised of $m + 1$ atoms. For each of the N molecules we tag an arbitrary atomic site and label its position vector $\mathbf{r}_i$, with $i = 1 \ldots N$. The position vectors of the remaining m atoms we write as $\mathbf{r}_{i,j} = \mathbf{r}_i + \mathbf{u}_{i,j}, j = 1 \ldots m$, with $\mathbf{u}_{i,j}$ the displacement of atom j on molecule i from the tagged atom $\mathbf{r}_i$. Accordingly a molecular configuration can be specified via a list of the N tagged and the $M = Nm$ non-tagged coordinates, $\mathbf{r}^N, \mathbf{u}^M$. The corresponding Boltzmann probability is

$$P_N(\mathbf{r}^N, \mathbf{u}^M) = \frac{e^{-\beta U(\mathbf{r}^N, \mathbf{u}^M)}}{Z_N} , \tag{1}$$

where $U(\mathbf{r}^N, \mathbf{u}^M)$ is the full interaction potential containing both intra and intermolecular terms and

$$Z_N = \int e^{-\beta U(\mathbf{r}^N, \mathbf{u}^M)} \mathrm{d}\mathbf{r}^N \mathrm{d}\mathbf{u}^M \tag{2}$$

is the N-molecule configurational integral.

Now define

$$\tilde{g}_N(\mathbf{r}^N, \mathbf{u}^M) \equiv \frac{P_N(\mathbf{r}^N, \mathbf{u}^M)}{P_N^{\mathrm{ig}}(\mathbf{r}^N)} \tag{3}$$

$$= V^N \frac{e^{-\beta U(\mathbf{r}^N, \mathbf{u}^M)}}{Z_N} , \tag{4}$$

where $P_N^{\mathrm{ig}}(\mathbf{r}^N) = V^{-N}$ is the probability of finding (within the same volume) a set of N structureless ideal gas particles in the same configuration as the tagged sites. We shall focus on the case in which the particle separations are all greater than the intermolecular interaction range R, i.e. $|\mathbf{r}_k - \mathbf{r}_l| > R, \ \forall k, l$. In this regime the molecules are non-interacting, so we can integrate out the internal molecular degrees of freedom (associated with the $\mathbf{u}_{i,j}$) to obtain the asymptotic value

$$f_N(V) \equiv \tilde{g}_N(\mathbf{r}^N) \quad |\mathbf{r}_k - \mathbf{r}_l| > R, \ \forall k, l \tag{5}$$

$$= \frac{(\Omega V)^N}{Z_N} \tag{6}$$

$$= \frac{Z_1^N}{Z_N} , \tag{7}$$

where Ω is the integral over the internal degrees of freedom of a single molecule (which is equal to $8\pi^2$ for a rigid molecule with no special symmetries) and Z_1 is the corresponding configurational integral.

The quantity $f_N(V) = Z_1^N / Z_N$ is central because it permits a direct calculation of molecular virial coefficients as will be shown below. A key feature is its dependence on the system volume. Specifically, although it has the low density limiting behaviour $\lim_{V \to \infty} f_N(V) = 1$, (because Z_N is dominated by configurations in which the N molecules are well separated) for finite system volume $f_N(V)$ deviates from unity. Clearly, however, determining $f_N(V)$ by simulation via eq. 7 is not a feasible proposition since it entails populating a $3N$-dimensional histogram for $P_N(\mathbf{r}^N)$ with sufficient statistics to yield precise probabilities. Fortunately, though, it turns out to be possible to determine $f_N(V)$ using only one-dimensional histograms. To see this, consider the quantity

$$g'_N(r_{\min}) \equiv \frac{P_N(r_{\min})}{P_N^{\mathrm{ig}}(r_{\min})} . \tag{8}$$

Here $r_{\min}$ is, for some configuration, the magnitude of that vector between a pair of the N tagged sites that is smaller than all other separation vectors. In the course of a simulation, one can easily accumulate histograms for $P_N(r_{\min})$ and $P_N^{\mathrm{ig}}(r_{\min})$ and thus form $g'_N(r_{\min})$. We note that $P_N^{\mathrm{ig}}(r_{\min})$ is particularly simple to measure because it simple involves repeatedly picking N random points within the box volume V and finding the shortest of the $N(N-1)/2$ pair separations.

Now clearly the regime in which $r_{\min} > R$ is identical to that in which $|\mathbf{r}_k - \mathbf{r}_l| > R, \ \forall k, l$. Moreover, since in this regime the microstates of the tagged particles are visited with equal probability $\Omega^N Z_N^{-1}$, while those of the ideal gas are visited with equal probability V^{-N}, it follows that the asymptotic value of $g'_N(r_{\min})$ is the same as that of $\tilde{g}_N(\mathbf{r}^N)$, i.e.

$$g'_N(r_{\min} > R) = f_N(V) . \tag{9}$$

Equation (9) provides a straightforward computational prescription for determining $f_N(V)$, which in turn permits the calculation of the virial coefficients for the molecular system. For instance from the virial cluster expansion (see Appendix) one finds that for $N = 2$ particles

$$B_2 = \frac{V}{2}\left(1 - \frac{Z_2}{Z_1^2}\right)$$

$$= \frac{V}{2}\left(1 - \frac{1}{f_2(V)}\right) , \tag{10}$$

Similarly for three particles one has

$$B_3 = \frac{V^2(Z_1^4 - 3Z_2 Z_1^2 - Z_3 Z_1 + 3Z_2^2)}{3Z_1^4}$$

$$= 4B_2^2 - 2B_2 V + V^2 \frac{[f_3(V) - 1]}{3f_3(V)} . \tag{11}$$

While for four particles one finds

$$B_4 = \frac{V^3}{8Z_1^6} \left(2Z_1^6 - 12Z_2Z_1^4 - 8Z_3Z_1^3 + \left(27Z_2^2 - Z_4\right)Z_1^2\right.$$

$$+12Z_2Z_3Z_1 - 20Z_2^3\big)$$

$$B_4 = \frac{1}{8} \left(-12B_2\left(V^2 - 6B_3\right) + 60B_2^2V - 12B_3V\right.$$

$$\left. -128B_2^3 + \left[1 - 1/f_4(V)\right]V^3\right) . \quad (12)$$

More generally, knowledge of $Z_i, i = 2, \ldots, m$ permits the calculation of the mth virial coefficient B_m.

It is noteworthy that the expressions Eq. 10- 12 for the virial coefficients depend only on the statistics of the tagged sites. This reflects the fact that molecular virial coefficients are intrinsically coarse-grained quantities. In practical terms, therefore, it is as straightforward to calculate virial coefficients for a complex molecule as for a simple monatomic one.

B. Isolating three-body interactions in coarse-grained effective models

The ability to measure second and third order virial coefficients in molecular systems provides a route to quantifying the role of three-body interactions in effective coarse-grained models. To appreciate this, consider the third virial coefficient B_3^{mol} of the fully detailed molecular system. This contains information on both two and three-body interactions that appear in the full effective potential[12]. In order to isolate the three-body contribution one can compare B_3^{mol} for the full molecular system with B_3^{pair}, the third virial of a system of $N = 3$ particles interacting via an effective pair potential (potential of mean force)[7]. Now if, by construction, both the full molecular model and the effective pair potential have the same value of B_2, then the difference $B_3^{\mathrm{mol}} - B_3^{\mathrm{pair}}$ clearly isolates the contribution of (non-additive) three-body interactions to B_3^{mol}.

Such a comparison is effected very naturally within our method because the function $g_2'(r_{\min})$ (which is just $g_2'(r)$ for two particles) not only provides an estimate of B_2, it also yields the effective pair potential:

$$\beta W^{\mathrm{pair}}(r) = -\ln[g_2'(r)/f_2(V)] . \quad (13)$$

Thus measurements of $g_2'(r)$ and thence $f_2(V)$ for some V can be used to determine $W^{\mathrm{pair}}(r)$[25]. A simulation of three particles interacting via this pair potential provides an estimate of B_3^{pair}, which can be compared with that arising from a simulation of three molecules.

C. Extension to colloid-polymer mixtures

The formalism for molecular systems can be readily adapted to mixtures in which the coarse-graining involves tracing out the degrees of freedom associated with one species. Common examples are molecules in solution and colloid-polymer mixtures. For definiteness we shall specialize to the latter case which, as noted above is often modelled as a highly size-asymmetrical mixture of spheres. The coarse-graining procedure integrates out the small particle degrees of freedom to yield an effective one component fluid of the large spheres. The statistical mechanics of these spheres is exactly described via an effective Hamiltonian[1]

$$H^{\mathrm{eff}} = H^0 + \Theta . \quad (14)$$

Here H^0 is the bare interaction between the large particles while Θ is a many-body contribution arising from the small particles which can in turn be written as a sum over n-body terms

$$\Theta = \sum_{n=1}^{\infty} \theta_n . \quad (15)$$

Such many-body terms arise from the coarse-graining procedure even when the underlying interactions are pairwise additive.

Now for a system of N large particles described by this effective Hamiltonian, the configurational statistics are given by

$$P_N(\mathbf{r}^N) = \frac{e^{-\beta H^{\mathrm{eff}}(\mathbf{r}^N)}}{Z_N} , \quad (16)$$

where

$$Z_N = \int e^{-\beta H^{\mathrm{eff}}(\mathbf{r}^N)} \mathrm{d}\mathbf{r}^N \quad (17)$$

is the partition function of the effective fluid of N-colloids.

So by analogy with the arguments of Sec. III A, when the large particles are all separated by a distance greater than the range R over which they interact (the lengthscale of which is set by the small particle diameter), one has

$$g_N'(\mathbf{r}^N) = f_N(V) \quad (18)$$

$$= \frac{V^N}{Z_N} , \quad (19)$$

where in the last equality we have set $Z_1 = V$ since the large particles have no internal degrees of freedom. Then by the same arguement as given in Sec. III A, one finds

$$g_N'(r_{\min}) = f_N(V), \quad r_{\min} > R \quad (20)$$

Generally speaking, the full many-body effective Hamiltonian is inaccessible due to the analytical and computational difficulties of calculating its form exactly. In

its absence, it is common practice in theoretical treatments to resort to a pair potential approximation, ie. to truncate the series for Θ (Eq. 15) at $n = 2$. For colloid-polymer mixtures the resulting pair potential is known as the depletion potential. To assess the neglect of three-body interactions in this approximation on the thermodynamics of the system, one can follow the strategy of Sec. III B and measure the difference $B_3^{\text{eff}} - B_3^{\text{dep}}$. To do so one first apples the method of Sec. III A in simulations of a system of $N = 3$ particles interacting via the depletion pair potential to yield B_3^{dep}. Next one simulates $N = 3$ large particles immersed in the sea of small ones (a task for which specialized algorithms may be required, see Sec. VI). But by *fiat*, the statistical mechanics of the large particles in such a simulation are just those of the effective system. Accordingly if in such a simulation one tags the large particles, then Eq. 19 together with Eqs. 10 and 11 provide estimates of B_3^{eff}.

IV. COMMENTARY

A. Optimization and limitations

Our method for estimating virial coefficients rests on measurements of the asymptote $f_N(V)$. Generally speaking, for a given computational expenditure, the numerical precision of the resulting estimates for B_N can be optimised by choosing as small a system volume V as possible consistent with maintaining access to the asymptotic regime of $g'_N(r_{\min})$. To appreciate this, consider the case of the absolute error in B_2. From Eq. (10) this is

$$\delta B_2 = \frac{V}{2f_2^2}\delta f_2 , \qquad (21)$$

showing that an absolute error δf_2 in f_2 is scaled up by a factor V. As far as the relative error is concerned one has

$$\frac{\delta B_2}{B_2} = \frac{\delta f_2}{f_2(f_2 - 1)} , \qquad (22)$$

which shows that this is sensitive to the magnitude of the finite-size 'signal' $f_2(V) - 1$. However, from Eq. (10),

$$f_2(V) - 1 = \frac{2B_2}{V - 2B_2} , \qquad (23)$$

and since B_2 is fixed by the model, this shows that in order to obtain a larger signal, it helps to choose a small V.

Similar arguments relate to B_N with $N > 2$, though here the absolute error grows like V^{N-1}, which implies that a large computational investment is required to access virial coefficients higher than the third. One is helped, however, if the interactions are short ranged since this allows access to the asymptotic regime of $g'_N(r_{\min})$ using small system volumes. We also note that for

systems with attractive interactions, the magnitude of $f_N(V) - 1$ is increased by lowering the temperature so that the molecules spend more time in close contact. Although at very low temperatures this effect could potentially result in poor statistics for estimates of $f_N(V)$, this problem can be easily surmounted by using biased (umbrella) sampling to enhance the sampling in the tail region of $P_N(r_{\min})$.

B. Radial distribution functions, tail effects and pair potentials

The radial distribution function $g(r)$ is a key structural characteristic of a fluid system and a common goal of simulations is to measure its form accurately. However, simulation estimates are necessarily based on a fixed finite number of particles N in a finite volume V. As is well known, in contrast to the true $g(r)$, the asymptote of the measured function (let us denote it $g_N(r)$) fails to approach unity[12,26–32]. This 'tail effect' complicates the extraction of structural and thermodynamic information from simulation measurements of $g_N(r)$ which has to be corrected by an empirical scaling procedure.

It is interesting to consider the behaviour of the asymptote of $g_N(r)$, in the limit of infinite volume so that $N/V \to 0$. In this limit, the asymptote differs from unity, i.e

$$\lim_{r,V\to\infty} g_N(r) \neq 1 . \qquad (24)$$

The finite-N dependence of the asymptote arises from the fact that the definition of $g(r)$ in terms of the two body distribution function is normalized using the density of an ideal gas of N rather than $N - 1$ particles[12]. This definition is followed in algorithmic prescriptions for measuring $g_N(r)$ by simulation[33,34]. However the considerations of Sec. III A suggests a better estimator for $g(r)$ that avoids this problem, namely:

$$g'_N(r) \equiv \frac{P_N(r)}{P_N^{ig}(r)} , \qquad (25)$$

where $P_N(r)$ is the probability of finding a particle a distance r from another particle (assumed to be at the origin) in the N particle system and $P_N^{ig}(r) = 4\pi r^2/V$. The asymptote of $g'_N(r)$ is unity in the limit $V \to \infty$, i.e.

$$\lim_{r,V\to\infty} g_N(r) = 1 \qquad (26)$$

for all N.

Now $g'_N(r)$ is simply related to the standard definition by

$$g'_N(r) = \frac{N}{N-1}g_N(r) . \qquad (27)$$

But while both $g'_N(r)$ and $g_N(r)$ will be identical in the thermodynamic limit in which $N, V \to \infty$, at fixed, finite number density N/V, $g'_N(r)$ can be expected to provide a superior estimator for finite N and V because it obviates the need to deal with corrections to the asymptote associated with finite N. Consequently, in simulations one only has to correct $g'_N(r)$ for finite-*volume* effects, and the associated degree of empirical scaling will thus be generally less than for $g_N(r)$.

The differences between the two estimators will of course be small in most situations because generally one deals with hundreds or thousands of particles. However when seeking to calculate pair potentials (which are defined in the limit of vanishing density), one considers only a pair of particles, $N = 2$. For this case, $g'(r) = 2g_2(r)$ – a stark difference. Since for a pair of particles $r_{min} = r$, this is just the situation considered in detail in Sec III A which sets out the relationship between the finite-V tail effect and the second virial coefficient.

C. Relationship to the Kirkwood-Buff integrals for mixtures

Although a slight digression, it is notable that a variation of our method for measuring the second virial coefficient provides a route to estimating the Kirkwood-Buff integrals which quantify the net affinity of a pair of species in a fluid mixture. For components i and j these integrals are defined

$$G_{ij} = \int_0^\infty (g_{ij}(r) - 1) 4\pi r^2 \mathrm{d}r , \qquad (28)$$

where $g_{ij}(r)$ is the partial radial distribution function.

Although for large numbers of particles the effects of finite N on $g_{ij}(r)$ are much less pronounced than for the case of $N = 2$ discussed above, the asymptote of $g_{ij}(r)$ will nevertheless typically differ significantly from unity in simulations. In practice this complicates accurate measurements of Kirkwood-Buff integrals[29,35,36].

It is therefore noteworthy that estimates of the Kirkwood-Buff integrals can be obtained without the need for integration by measuring the asymptotic value

$$f_{ij}(V) \equiv \lim_{r_{ij} \to \infty} g'_{ij}(r_{ij}) \qquad (29)$$

where

$$g'_{ij}(r_{ij}) = \frac{P(r_{ij})}{P^{ig}(r_{ij})} , \qquad (30)$$

with $P(r_{ij})$ the probability of finding a particle of species j a distance r_{ij} from a particle of species i (the latter assumed to be at the origin) and $P^{ig}(r_{ij}) = 4\pi r^2/V$.

If one inserts Eq. 30 into Eq. 28 instead of $g_{ij}(r_{ij})$ one finds $G_{ij} = 0$ always. The reason for this is a finite-size effect, namely the fact that the asymptote $f_{ij}(V)$ of

$g'_{ij}(r_{ij})$ differs from unity. In order to obtain the correct integral, one therefore has to multiply g'_{ij} by a factor $f_{ij}(V)^{-1}$. It thus follows that the Kirkwood-Buff integral can be written in terms of the measured asymptote $f_{ij}(V)$, ie.

$$G_{ij} = V \left(\frac{1}{f_{ij}(V)} - 1 \right) , \qquad (31)$$

which is analogous to Eq. 10.

V. ILLUSTRATION AND TEST

In order to both illustrate and test the method, it is instructive to use it to estimate the first few virial coefficients of a single component system of hard spheres, for which exact values of virial coefficients are known. Considering first the calculation of B_2 for hard spheres, here one has $N = 2$ and hence $r_{\min} = r$. Fig. 2(a) plots the measured forms of $P_2(r)$, $P_2^{ig}(r)$ and their ratio $g'_2(r)$ obtained by a simple Monte Carlo simulation of a pair of particles in a periodic box of volume $V = (2.5\sigma)^3$, with σ the hard sphere diameter. For this simple interaction potential, the limiting value of $g'_2(r)$ pertains for all $r > \sigma$. Note also that both the probability distributions $P_2(r)$ and $P_2^{ig}(r)$ show a maximum as $r_{\min}$ increases. This is a finite-size effect arising from the fact that the available volume at large $r_{\min}$ decreases due to the cubic box geometry. Nevertheless $g'_2(r)$ remains flat inside this regime because the contribution from this finite-size effect exactly cancels when forming the ratio of the two distributions.

In general one can estimate $f_N(V)$ visually, or from a fit. However, we have found that a particularly accurate measure results from the ratio of integrals

$$f_N(V) = \frac{\int_{r_l}^{r_u} P_N(r_{\min}) \mathrm{d}r_{\min}}{\int_{r_l}^{r_u} P_N^{\mathrm{ig}}(r_{\min}) \mathrm{d}r_{\min}} , \qquad (32)$$

where r_l is some value of $r_{\min}$ for which $g'(r_{\min})$ can be considered to have first reached its limiting value, and r_u is the largest value of $r_{\min}$ for which data has been accumulated, which will typically be half the simulation box diagonal length. It should be emphasized that in practice, eq. (32) is evaluated simply from a count of entries in the respective histograms for $P_N(r_{\min})$ and $P_N^{\mathrm{ig}}(r_{\min})$–no numerical quadrature is performed. In this way we find (taking $r_l = \sigma$) that $B_2 = 2.09441(6)\sigma^3$, to be compared with the exact value $B_2 = 2\pi\sigma^3/3 = 2.094395\sigma^3$.

Turning next to the third virial coefficient B_3, here one has $N = 3$ hard spheres and MC simulations of a trio of particles in a box of volume $V = (3.5\sigma)^3$ yields the forms of $P_3(r_{\min})$, $P_3^{ig}(r_{\min})$ and $g'_3(r_{\min})$ shown in Fig. 2(b). Again for this potential, $g'_3(r_{\min})$ reaches its limiting value immediately for $r_{\min} > \sigma$ and we find via
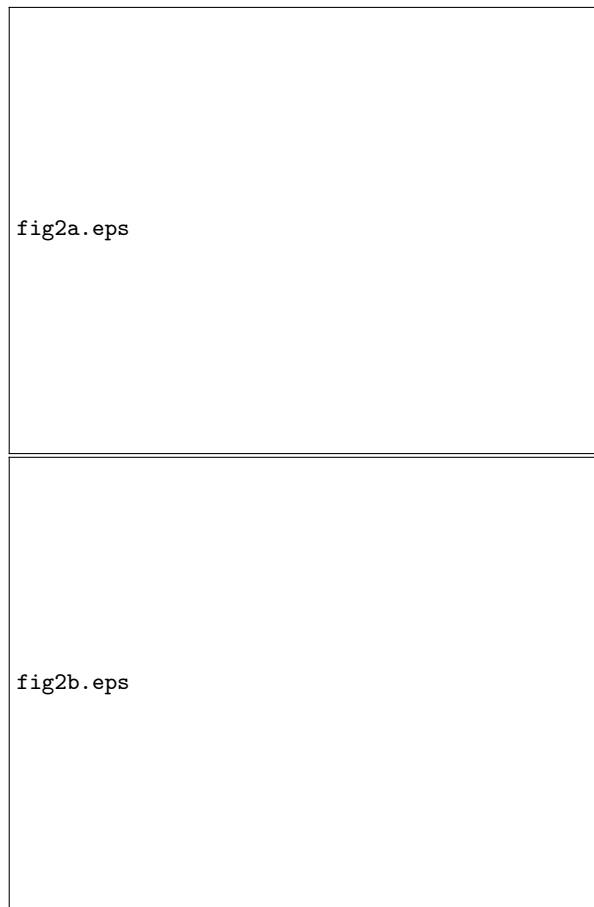
FIG. 2. **(a)** Simulation estimates of $P_2(r)$, $P_2^{ig}(r)$ and their ratio $g_2'(r)$ for hard spheres as obtained in an MC simulation with a periodic box of volume $V = (2.5\sigma)^3$. **(b)** Estimates of $P_3(r_{\min})$, $P_3^{ig}(r_{\min})$ and their ratio $g_3'(r_{\min})$ obtained in MC simulations with a periodic box of size $V = (3.5\sigma)^3$.

eq. (11), that $B_3 = 2.7418(4)\sigma^6$. This is to be compared with the exact value of $B_3 = 5\pi^2\sigma^6/18 = 2.741557\sigma^6$.

Finally, we consider B_4, which we have measured for a system of size $V = (3.5\sigma)^3$. The measured value of f_4 together with Eq. 12 implies that $B_4 = 2.629(22)\sigma^9$ to be compared with the exact value[37] of $2.6362\ldots\sigma^9$.

VI. APPLICATION I: THREE-BODY INTERACTIONS IN HIGHLY SIZE-ASYMMETRICAL FLUID MIXTURES

Having validated our method, we now turn to a more challenging problem, namely that of determining the second and third virial coefficients of the effective Hamiltonian for highly size asymmetrical mixtures.

When colloids are immersed in a sea of small particles such as polymers or much smaller colloids, the small particles mediate effective colloidal interactions. In the simplest case in which all particles are hard, the effective interaction arises solely from entropic effects and results in an enhanced attraction between the colloids known as the depletion interaction which acts on a length scale set by the small particle diameter. More generally the nature of the effective interaction can depend sensitively on the detailed form of the interactions between the small particles and the large ones.

As described in Secs. I and III C, theoretically one would like to describe such a system in terms of a single component model of colloids interacting according to a many-body effective Hamiltonian. This Hamiltonian would in principle provide an exact representation of the actual mixture and contain two-body, three-body, etc terms. However, many-body terms can be difficult to calculate in practice and thus one usually focuses on the two-body contribution in the expectation that (at least for small q), many-body effects should be small.

A commonly studied model treats the colloids as big hard spheres of diameter σ_b and the small particles as hard spheres of diameter σ_s. The size ratio is then expressed as $q \equiv \sigma_s/\sigma_b$. In the two-body approximation, the effective Hamiltonian between the colloids is written as a sum over pair interactions:

$$H^{\text{eff}} \approx \sum_{i,j}[\phi(r_{ij}) + W(r_{ij})]\,, \tag{33}$$

where $\phi(r_{ij})$ is the hard sphere interaction between a pair of colloids whose centers are separated by a distance r_{ij}, while $W(r_{ij})$ is the depletion pair potential, whose form depends on the small particle volume fraction and model details such as whether or not the big-small interaction is additive. Typically one imagines that the small particles are in equilibrium with a reservoir so that $W(r)$ is parameterized in terms of the *reservoir* volume fraction η_s^r.

Depletion potentials have been estimated using both theory and simulation.[25,38–51] for a variety of models such as additive and non-additive hard spheres. Calculations of the phase behaviour of systems interacting through depletion potentials has revealed interesting features such as a metastable fluid-fluid phase separation at high values of η_s^r[1,3,52] in additive hard spheres. However since simulations of depletion potentials neglect the many-body forces that occur in the full mixture, the question as to whether such effects actually occur in the full mixture is somewhat moot[53,54].

In view of this it is desirable to have techniques for quantifying the effects of neglecting many-body interactions when employing depletion potentials. Let us focus on three-body interactions, which are (typically) the dominant many-body effect. As discussed in Sec. III B, one systematic way to study three-body effects in this system (there are others[55–57]) is to calculate the third virial coefficient B_3^{eff} for the full effective fluid and compare it with the corresponding value B_3^{dep} arising from a simulation of three particles interacting via the appropriate depletion potential[58]. This comparison will directly probe the extent to which the net interaction between a pair of large hard spheres particles in the full mixture

is influenced by the proximity of a third large sphere which modulates the small particle density distribution. By contrast for a trio of particles interacting through the two-body depletion potential, no such effect exists by definition.

Below we describe how one can perform this comparison by combining the method described in Sec. III for estimating virial coefficients, with state-of-the-art simulation techniques for dealing with highly size asymmetrical fluid mixtures.

A. Computational procedure for determining B_3^{eff} and B_3^{dep}

In order to obtain estimates for both B_3^{eff} and B_3^{dep} in highly size asymmetrical mixtures, we deploy the geometrical cluster algorithm (GCA)[59,60]. This is a collective updating Monte Carlo scheme which provides efficient relaxation at practically any particle size ratio provided the overall volume fraction is not too high. Our implementation reproduces conditions considered in many experimental and theoretical studies of colloids, in that we treat the small particles grand canonically so that their properties are parameterized in terms of the reservoir volume fractions η_s^r. Transfers of small particles are effected using a standard grand canonical approach[33]. However to utilize this ensemble one needs to know accurately the chemical potential corresponding to a given η_s^r. For some types of small particle fluid, such as hard spheres, this relationship is independently known. Otherwise, it has to be determined in a separate simulation.

Using the GCA, we can study the statistical mechanics of either a pair or a triple of big particles in a sea of small ones. The procedure for implementing the strategy of Sec. III B is as follows

(i) From simulations of $N = 2$ big particles, measure the form of $g_2'(r)$ at some prescribed η_s^r. This yields the value of $B_2^{\text{eff}}(\eta_s^r)$ via eq. (10).

(ii) Use the form of $g_2'(r)$ obtained in (i) to estimate the depletion potential as

$$\beta W(r|\eta_s^r) = -\ln[g_2'(r)/f_2(V)]$$

(iii) Next simulate three big particles at the same value of η_s^r and measure $g_3'(r_{\min})$. Together with the estimate of $B_2^{\text{eff}}(\eta_s^r)$ obtained in (i), this provides an estimate for $B_3^{\text{eff}}(\eta_s^r)$ via eq. (11).

(iv) Finally perform a simple MC simulation of three particles interacting via the appropriate depletion potential $W(r|\eta_s^r)$ as obtained in (ii) to determine the form of $\tilde{g}_3(r_{\min})$. Together with the estimate of $B_2^{\text{eff}}(\eta_s^r) = B_2^{\text{dep}}(\eta_s^r)$ obtained in (i), this gives the third virial coefficient $B_3^{\text{dep}}(\eta_s^r)$ via eq. (11).

In what follows, we detail our measurements of $B_3^{\text{eff}}(\eta_s^r)$ and $B_3^{\text{dep}}(\eta_s^r)$ for two models of highly size-asymmetrical mixtures, namely the Asakura-Oosawa model and a system of additive hard spheres.

B. Asakura-Oosawa model

The Asakura-Oosawa (AO) model describes colloidal hard-spheres in a solvent of non-interacting particles modelling ideal polymer that have a hard-particle interaction with the colloids[61,62]. Owing to its extreme non-additivity, the model is somewhat analytically tractable. Specifically, the exact form of the depletion pair potential is known[62] to be

$$\beta W_{\text{AO}}(r) = \begin{cases} -\eta_s^r \frac{(1+q)^3}{q^3} \left[1 - \frac{3r}{2\sigma_b(1+q)} + \frac{r^3}{2\sigma_b^3(1+q)^3} \right] , & \sigma_b < r < \sigma_b + \sigma_s \\ 0, & r \geq \sigma_b + \sigma_s , \end{cases} \tag{34}$$

where σ_s is the 'polymer' diameter, i.e. the colloid-polymer pair potential is infinite for $r < (\sigma_b + \sigma_s)/2$. This fact obviates the need to implement steps (i) and (ii) in the procedure of Sec. VI A. Another interesting aspect of the model is that owing to the lack of polymer-polymer interactions, the effective potential contains no many-body interactions for size ratios $q < 0.1547$[63]. This renders the model an excellent proving ground for testing the sensitivity of our approach.

Fig. 3 shows our estimates of $B_3^{\text{eff}}(\eta_s^r)$ and $B_3^{\text{dep}}(\eta_s^r)$ for three size ratios, $q = 0.5, 0.25, 0.154$ obtained using the methodology of Sec. III. The estimates of B_3 are all normalized by the value for pure hard spheres which pertains in the limit $\eta_s^r \to 0$, and curves for the various q are shifted for clarity. One expects that many body effects, quantified by the difference between $B_3^{\text{eff}}(\eta_s^r)$ and $B_3^{\text{dep}}(\eta_s^r)$ should increase with η_s^r and this is indeed the case, as our data show. Furthermore, the differences should diminish with decreasing q and have disappeared by $q = 0.154$. Again this is confirmed by our data.

FIG. 3. Comparison for size ratios $q = 0.5, 0.25, 0.154$ and various η_s^r of the measured values of B_3 arising from the simulation of the full two component AO model $(B_3^{\mathrm{eff}}(\eta_s^r))$, and a three particle system interacting via the AO depletion potential of eq. (34) $(B_3^{\mathrm{dep}}(\eta_s^r))$. Lines are guides to the eye and statistical uncertainties are smaller than the symbol sizes. To aid visibility, the curves for $q = 0.25$ and $q = 0.5$ have been shifted vertically by 0.5 and 1.0 respectively. Reproduced from Ashton, Wilding, Phys. Rev. E **89**, 031301 (2014). Copyright (2014) by the American Physical Society.

C. Additive hard sphere mixtures

Turning now to the more challenging system of additive hard spheres, here the GCA permits access to a much more limited range of η_s^r than for the AO model, and beyond $\eta_s^r = 0.2$ relaxation times become prohibitive. In contrast to the AO model the depletion pair potential is not known exactly for the additive mixtures, so we measure it in a simulation of two large particles as described in Sec. VI A. For this system the reservoir chemical potential $\mu(\eta_s^r)$ of the small particles is obtained from the equation of state of Kolafa *et al* [64], which we have checked provides a highly accurate representation of grand canonical ensemble simulation data.

Although three-body interactions are always present in principle, our results shown in fig. 4, indicate that within this more limited range of η_s^r, they are negligibly small for $q = 0.2$ and $q = 0.1$. This finding suggests that for applications at low to moderate η_s^r and small q it is safe to use depletion potentials for additive hard spheres. Unfortunately, we are unable to provide indications of the scale of three-body interactions in the regime of putative phase separation[25] which lies above $\eta_s^r = 0.3$. To do so would require a more efficient simulation algorithm for dealing with mixture of additive hard spheres than is currently available.

Compared to the AO model the statistical noise on our estimates of B_3 are greater for additive hard spheres, particularly at larger q. There are a number of factors contributing to this extra noise: The interaction range is longer due to correlations in the solvent (as shown in fig.

4(a)), while the overall interaction strength is weaker for a given η_s^r. We therefore require a larger box to access the asymptotic regime and the value of the finite-size signal $f(V) - 1$ will be smaller, leading to some loss of precision as described in Sec. IV A. This is particularly apparent at larger q as seen in fig. 4(b). The lowest statistical noise is for $q = 0.1$ where we were able to use a smaller box, $L = 3.5\sigma$, as opposed to $L = 4\sigma$ for the other q values. In addition, because the GCA algorithm is considerably less efficient for hard sphere solvents, the amount of statistics we can gather is much less compared to the AO model for equal computing time.
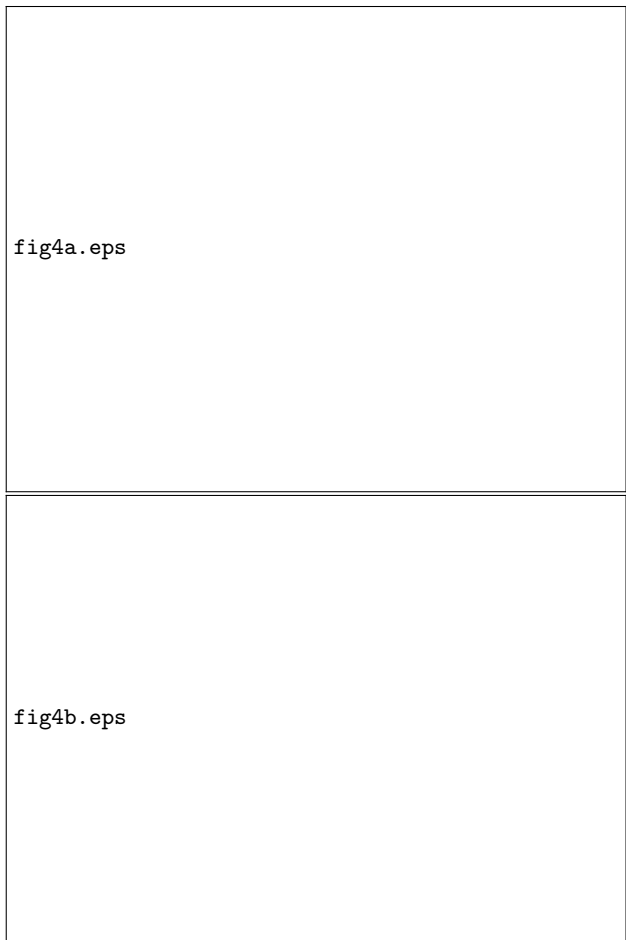

FIG. 4. **(a)** Simulation estimates of $P_3(r_{\min})$, $P_3^{ig}(r_{\min})$ and their ratio $g_3'(r_{\min})$ as obtained in an MC simulation of additive hard spheres for $q = 0.2$ and $\eta_s^r = 0.1$. The volume of the periodic box is $V = (3\sigma)^3$. **(b)** Comparison for size ratio $q = 0.1$, 0.2 and 1/3 and various η_s^r of the measured values of B_3 arising from the simulation of the full two component additive hard sphere model $[B_3^{\mathrm{eff}}(\eta_s^r)]$, and a three particle system interacting via the depletion potential $[B_3^{\mathrm{dep}}(\eta_s^r)]$. The curves for $q = 0.2$ and $q = 1/3$ have been shifted vertically by 0.5 and 1.0 respectively.

VII. APPLICATION II: THREE-BODY INTERACTIONS IN STAR POLYMERS

As a further application of our method, we have used it to quantify the scale of three-body interactions in coarse-grained models for star polymers in implicit solvent. We model each polymer in terms of a core particle which is functionalised by a number of linear polymer chains each comprising n monomers. Bonded monomers interact via a FENE spring[65], while non-bonded monomers experience a Lennard-Jones (LJ) potential. Using the Lammps Molecular Dynamics package[66] we have studied various combination of functionality and chain length n. Our aim was to determine how these parameters affect the size of the three-body interactions.

Varying functionality and arm chain length leads to overall changes in the balance of attraction and repulsion between molecules ie. to the second virial coefficient B_2. Accordingly, in order to isolate the influence of three-body interactions we have, for each combination of functionality and n studied, measured B_3 at a fixed value of B_2. This was achieved by using histogram reweighting[67] to extrapolate our measured data for $g_2'(r)$ with respect to temperature such to to precisely locate that temperature for which B_2 matches a prescribed value. This value was chosen to correspond to a moderately attractive system, corresponding to a somewhat poor solvent[68].

The procedure for measuring the size of three-body interactions via virial coefficients is similar to that outlined for the colloid-polymer mixtures, except that the tagged particles are now taken to be the set of core atoms. The pair potential is the potential of mean force (pmf) which is obtained in a simulation of two stars. We then simulate three particles interacting via this potential to obtain B_3^{pmf}. This we compare with B_3^{star}, measured in a simulation of $N = 3$ star polymers. An example plot of $g_3'(r_{\mathrm{min}})$ is shown in Fig. 5 measured for a system of three star polymers each having 7 arms of length $n = 10$.

Our collected results are shown in Fig. 6 and reveal considerable discrepancies between B_3^{pmf} and B_3^{star}, particularly for small values of the functionality and the arm length. Clearly the disparity is such that one should expect a quite different equation of state (as well as other thermodynamic quantities) to arise from the coarse-grained system described by the pmf compared to the full model.

The important role of many-body effects in this system arises from the ability of the polymers to occupy the same volume. When two polymers overlap, the local density of the resulting composite particle is much greater than for a single polymer. Accordingly a third polymer is much less likely to overlap with the first two due to short ranged monomeric repulsions. However, this effect is completely neglected in the pair potential framework for which the degree of attraction is purely additive. This finding should be relevant to many other types of polymer-based soft particles, including cluster forming amphiphilic dendrimers[69].

FIG. 5. Example of the form of $g_3'(r_{\mathrm{min}})$ obtained in a study of three 7-armed stars with arm chain length $n = 10$. The box volume is $V = (40\sigma)^3$. The inset focuses on the asymptotic region.
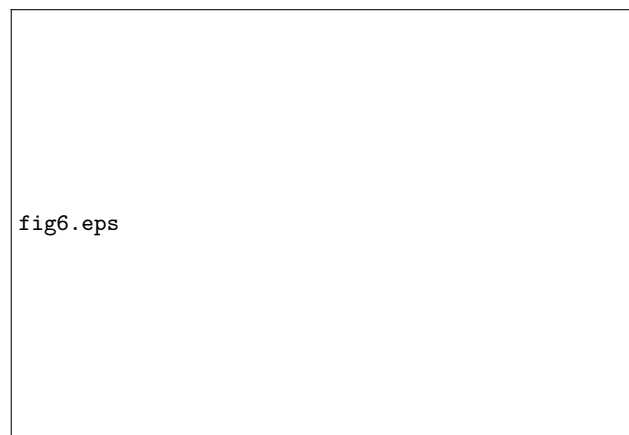
FIG. 6. Estimates of the dimensionless third virials B_3^{pmf}/B_2^2 and $B_3^{\mathrm{star}}/B_2^2$ versus functionality for various chain lengths n. Volumes ranged from $V = (20\sigma)^3$ to $V = (40\sigma)^3$, large enough to access the limiting behaviour of $g_3'(r_{\mathrm{min}})$. Bonded monomers interact via a FENE potential with parameters $K = 30.0\epsilon/\sigma^2, R_0 = 1.5\sigma$[65]. The LJ potential was truncated and shifted at $r = 2.5\sigma$. In all cases T is chosen to yield $B_2 = -3321\sigma^3$. Errors are comparable with symbol sizes. Reproduced from Ashton, Wilding, Phys. Rev. E **89**, 031301 (2014). Copyright (2014) by the American Physical Society.

VIII. SUMMARY

We have proposed a technique for studying three-body interactions in coarse-grained models for complex fluids. The method rests on measurements, for $N = 2$ and $N = 3$ particles, of the asymptote of a simple-to-measure structural function $g_N'(r_{\mathrm{min}})$. For finite simulation box volumes this asymptote yields the ratio of configurational integrals Z_1^N/Z_N, which in turn provides estimates of virial coefficients. Comparison of the measured value of the third virial coefficient of the full system with that of

an approximate coarse-grained representation (involving only pair potentials) provides information on the scale of three-body interactions in the effective Hamiltonian. Since the method is based solely on structural information, it can be utilized with any simulation scheme capable of generating equilibrium configurations.

Our approach follows the partition function route to virial coefficients. Consequently it struggles to access high order virial coefficient for reasons discussed in Sec. IV A. For simple fluids other methods based on the Mayer function route (such as the MSM) allow one to reach higher order virial coefficients. However for calculating low order virials of complex fluids the present method appears to be a useful tool. This is because it focuses attention on the configurational statistics of a single atom in the molecule; there is no need to explicitly integrate over molecular conformations. Being based on structural information it can also be applied in situations where the Mayer route fails, namely effective models for mixtures that arise from tracing out the degrees of freedom of one species.

We have applied the method to calculate the contribution of three-body interactions to the third virial coefficient of the effective Hamiltonian in size asymmetrical hard sphere mixtures which serves as a prototype model for colloid-polymer mixtures or molecular solutions. Using the geometrical cluster algorithm, we were able to scan a wide range of size ratios q and small particle reservoir volume fractions η_s^r. In the Asakura-Oosawa model at large q and large η_s^r three-body effects were found to be substantial; for example at $q = 0.5$ and $\eta_s^r = 0.5$, we find $B_3^{\mathrm{eff}}/B_3^{\mathrm{dep}} \approx 3$. However, as expected on decreasing q, the differences diminish rapidly and, for $q = 0.154$, were found to be identically zero within numerical uncertainty for all η_s.

Compared with the AO model, additive hard spheres present a significantly greater computational challenge. The range of η_s^r accessible to the cluster algorithm is much smaller than the AO model, being limited to $\eta_s^r < 0.2$. Our results indicate that within this more limited range of η_s^r, three-body interactions are negligibly small for $q = 0.2$ and $q = 0.1$. This finding suggests that for applications at low to moderate η_s^r and small q it is safe to use depletion potentials for additive hard spheres.

Finally, our study of star polymers modelled as soft effective spheres, revealed large three-body contributions to the effective potential which are neglected in the pair potential picture. It was argued that it is the ability of such molecules to substantially overlap which leads to the failure of the pair potential approach in such systems.

Appendix A: Virial coefficients in terms of configurational integrals

Here we outline the derivation of the relationships between the virial coefficients, B_N, and the partition functions, following the approach of Hill[24]. The starting point is the grand partition function for a monodisperse assembly of particles

$$\Omega = \sum_{N=1}^{\infty} \frac{1}{N!} z^N Z_N \,. \tag{1}$$

Here $z = e^\mu$, is the fugacity and Z_N is the N-particle configurational integral:

$$Z_N = \int_{\mathbf{r}^N} \mathrm{d}\mathbf{r}^N \exp\left(-\beta H(\mathbf{r}^N)\right) \,. \tag{2}$$

The pressure is related to Ω by

$$\beta PV = \log \Omega \,, \tag{3}$$

and we can take derivatives of the grand partition function to get

$$\langle N \rangle = \rho V = z \frac{\partial \log \Omega}{\partial z} \,. \tag{4}$$

By taking functional derivatives we can expand Ω as a series in the fugacity:

$$\frac{\log \Omega}{V} = \beta P = \sum_{j=1}^{\infty} b_j z^j \,, \tag{5}$$

and also the density

$$\rho = \sum_{j=1}^{\infty} j b_j z^j \,. \tag{6}$$

The coefficients, b_j, are the cluster integrals, which are related[24] to the semi-invariants

$$j! V b_j = j! \sum_{\mathbf{n}} \left((-1)^{s_j} s_j! \prod_{k=1}^{j} \left[\frac{(Z_k/k!)^{n_k}}{n_k!} \right] \right) \tag{7}$$

where $s_j = (\sum_{i=1}^{j} n_i) - 1$ and the first sum is over all sets of zero or positive integers, $\mathbf{n}$, such that $\sum_i i n_i = j$. Thus for $j = 1$ the only possibility is $n_1 = 1$, while for $j = 2$, one has $n_1 n_2 = 01$ and 20, and for $j = 3$ the possibilities are $n_1 n_2 n_3 = 001$, 110 and 300. The resulting invariants are

$$1!Vb_1 = Z_1 \tag{8}$$
$$2!Vb_2 = Z_2 - Z_1^2 \tag{9}$$
$$3!Vb_3 = 2Z_1^3 - 3Z_2Z_1 + Z_3 \tag{10}$$
$$4!Vb_4 = -6Z_1^4 + 12Z_2Z_1^2 - 4Z_3Z_1 - 3Z_2^2 + Z_4 \tag{11}$$

To obtain virial coefficients, one starts with the virial expansion of the pressure.

$$\beta P = \rho + \sum_{N=2}^{\infty} B_N \rho^N . \tag{12}$$

Then substituing Eq. 6 into Eq. 12 and equating coeffi-

cients in z with those from Eq. 5 yields the virial coefficients in terms of the cluster integrals:

$$B_1 = 1 \tag{13}$$
$$B_2 = -\frac{b_2}{b_1^2} \tag{14}$$
$$B_3 = \frac{4b_2^2 - 2b_1b_3}{b_1^4} \tag{15}$$
$$B_4 = \frac{-20b_2^3 + 18b_1b_3b_2 - 3b_1^2b_4}{b_1^6} \tag{16}$$

Finally, substituting for configurational integrals, one finds

$$B_2 = \frac{1}{2}V\left(1 - \frac{Z_2}{Z_1^2}\right) \tag{17}$$
$$B_3 = \frac{V^2\left(Z_1^4 - 3Z_2Z_1^2 - Z_3Z_1 + 3Z_2^2\right)}{3Z_1^4} \tag{18}$$
$$B_4 = \frac{V^3\left(2Z_1^6 - 12Z_2Z_1^4 - 8Z_3Z_1^3 + \left(27Z_2^2 - Z_4\right)Z_1^2 + 12Z_2Z_3Z_1 - 20Z_2^3\right)}{8Z_1^6} \tag{19}$$

[1] M. Dijkstra, R. van Roij, and R. Evans, Phys. Rev. E **59**, 5744 (1999).
[2] A. A. Louis, P. G. Bolhuis, J. P. Hansen, and E. J. Meijer, Phys. Rev. Lett. **85**, 2522 (2000).
[3] J. Largo and N. B. Wilding, Phys. Rev. E **73**, 036115 (2006).
[4] H. N. W. Lekkerkerker and R. Tuinier, *Colloids and the Depletion Interactions*, Lecture Notes in Physics, Vol. 833 (Springer, Berlin / Heidelberg, 2011).
[5] A short report on this work has appeared elsewhere[70].
[6] G. D'Adamo, A. Pelissetto, and C. Pierleoni, Soft Matter **8**, 5151 (2012).
[7] G. D'Adamo, A. Pelissetto, and C. Pierleoni, J. Chem. Phys. **136**, 224905 (2012).
[8] K. R. S. Shaul, A. J. Schultz, and D. A. Kofke, Collect. Czech. Chem. Commun. **75**, 447 (2010).
[9] K. R. S. Shaul, A. J. Schultz, and D. A. Kofke, J. Chem. Phys. **135**, 124101 (2011).
[10] R. Hellmann and E. Bich, J. Chem. Phys. **135**, 084117 (2011).
[11] A. J. Masters, J. Phys: Condens. Matter **20**, 283102 (2008).
[12] J. P. Hansen and I. R. McDonald, *Theory of Simple Liquids* (Academic, London, 2006).
[13] L. R. Pratt, J. Chem. Phys. **77**, 979 (1982).
[14] B. Li, N. Madras, and A. Sokal, *Journal of Statistical Physics*, **80**, 661 (1995).
[15] S. Labík, J. Gabrielová, H.and Kolafa, and A. Malijevský, Mol. Phys. **101**, 1139 (2003).
[16] J. K. Singh and D. A. Kofke, Phys. Rev. Lett. **92**, 220601 (2004).
[17] A. J. Schultz and D. A. Kofke, Mol. Phys. **107**, 2309 (2009).
[18] H. M. Kim, A. J. Schultz, and D. A. Kofke, Fluid Phase Equilibria **351**, 69 (2013).
[19] S. Caracciolo, B. M. Mognetti, and A. Pelissetto, J. Chem. Phys. **125**, 094903 (2006).
[20] S. Caracciolo, B. M. Mognetti, and A. Pelissetto, Macromol. Theor. Simul. **17**, 67 (2008).
[21] K. Shida, A. Kasuya, K. Ohno, Y. Kawazoe, and Y. Nakamura, J. Chem. Phys. **126**, 154901 (2007).
[22] F. Randisi and A. Pelissetto, J. Chem. Phys. **139**, 154902 (2013).
[23] C. Vega, J. M. Labaig, L. G. MacDowell, and E. Sanz, J. Chem. Phys. **113**, 10398 (2000).
[24] T. Hill, *Statistical Mechanics: Principles and Selected Applications Principles and Selected Applications* (Dover Publications Inc., 1988).
[25] D. Ashton, N. Wilding, R. Roth, and R. Evans, Phys. Rev. E **84**, 061136 (2011).
[26] J. L. Lebowitz and J. K. Percus, Phys. Rev. **122**, 1675 (1961).
[27] J. L. Lebowitz and J. K. Percus, Phys. Rev. **124**, 1673 (1961).

[28] J. J. Salacuse, A. R. Denton, and P. A. Egelstaff, Phys. Rev. E **53**, 2382 (1996).

[29] A. Perera, L. Zoranić, F. Sokolić, and R. Mazighi, J. Mol. Liq. **159**, 52 (2011).

[30] B. Kezic and A. Perera, J. Chem. Phys. **137**, 014501 (2012).

[31] J. Kolafa, S. Labík, and A. Malijevský, Mol. Phys. **100**, 2629 (2002).

[32] K. Koga and B. Widom, J. Chem. Phys. **138**, 114504 (2013).

[33] D. Frenkel and B. Smit, *Understanding Molecular Simulation* (Academic, San Diego, 2002).

[34] M. P. Allen and D. J. Tildesley, *Computer Simulation of Liquids* (Oxford U.P., 1987).

[35] P. Krüger, S. K. Schnell, D. Bedeaux, S. Kjelstrup, T. J. H. Vlugt, and J.-M. Simon, J. Phys. Chem. Lett. **4**, 235 (2013).

[36] E. Matteoli and L. Lepori, J. Chem. Soc., Faraday Trans. **91**, 431 (1995).

[37] N. Clisby and B. M. McCoy, J. Stat. Phys. **114**, 1343 (2004).

[38] B. Götzelmann, R. Evans, and S. Dietrich, Phys. Rev. E **57**, 6785 (1998).

[39] R. Roth, R. Evans, and S. Dietrich, Phys. Rev. E **62**, 5360 (2000).

[40] R. Roth, R. Evans, and A. A. Louis, Phys. Rev. E **64**, 051202 (2001).

[41] A. A. Louis and R. Roth, J. Phys.: Condens. Matter **13**, L777 (2001).

[42] A. A. Louis, P. G. Bolhuis, E. J. Meijer, and J. P. Hansen, J. Chem. Phys. **117**, 1893 (2002).

[43] A. A. Louis, E. Allahyarov, H. Löwen, and R. Roth, Phys. Rev. E **65**, 061407 (2002).

[44] R. Roth and R. Evans, EPL **53**, 271 (2001).

[45] S. B. Yuste, A. Santos, and M. L. de Haro, J. Chem. Phys. **128**, 134507 (2008).

[46] S. Amokrane, A. Ayadim, and J. Malherbe, J. Chem. Phys. **123**, 174508 (2005).

[47] A. Ayadim and S. Amokrane, Phys. Rev. E **74**, 021106 (2006).

[48] M. Oettel, Phys. Rev. E **69**, 041404 (2004).

[49] M. Oettel, H. Hansen-Goos, P. Bryk, and R. Roth, Euro. Phys. Lett. **85**, 36003 (2009).

[50] V. Boţan, F. Pesth, T. Schilling, and M. Oettel, Phys. Rev. E **79**, 061402 (2009).

[51] D. J. Ashton, V. Sánchez-Gil, and N. B. Wilding, J. Chem. Phys. **139**, 144102 (2013).

[52] B. Rotenberg, J. Dzubiella, J. P. Hansen, and A. A. Louis, Mol. Phys. **102**, 1 (2004).

[53] Barrat, J.L. and Hansen, J.P., J. Phys. France **47**, 1547 (1986).

[54] M. L. de Haro, C. Tejero, and A. Santos, J. Chem. Phys **138**, 161104 (2013).

[55] D. Goulding and S. Melchionna, Phys. Rev. E **64**, 011403 (2001).

[56] J. Malherbe and S. Amokrane, Mol. Phys. **99**, 355 (2001).

[57] S. Amokrane, A. Ayadim, and J. G. Malherbe, J. Phys: Condens. Matter **15** (2003).

[58] Note that neither of these quantities is to be confused with the third virial coefficient of the full mixture[71], which is a quantity which treats small and large particles on an equal footing.

[59] C. Dress and W. Krauth, J. Phys. A **28**, L597 (1995).

[60] J. Liu and E. Luijten, Phys. Rev. Lett. **92**, 035504 (2004).

[61] S. Asakura and F. Oosawa, J. Chem. Phys. **22**, 1255 (1954).

[62] S. Asakura and F. Oosawa, J. Polym. Sci. **33**, 183 (1958).

[63] M. Dijkstra, J. Brader, and R. Evans, J. Phys: Condens. Matter **11**, 10079 (1999).

[64] J. Kolafa, S. Labík, and A. Malijevský, Phys. Chem. Chem. Phys. **6**, 2335 (2004).

[65] K. Kremer and G. S. Grest, J. Chem. Phys. **92**, 5057 (1990).

[66] S. Plimpton, J. Comp. Phys. **117**, 1 (1995).

[67] A. M. Ferrenberg and R. H. Swendsen, Phys. Rev. Lett. **61**, 2635 (1988).

[68] Although we choose this regime as a test for our method, it should be noted that coarse-grained models which treat polymers as monatomic particles are predicted to become thermodynamically unstable in the poor solvent regime for low concentrations[72,73].

[69] D. A. Lenz, R. Blaak, C. N. Likos, and B. M. Mladek, Phys. Rev. Lett. **109**, 228301 (2012).

[70] D. J. Ashton and N. B. Wilding, Phys. Rev. E **89**, 031301 (2014).

[71] E. Enciso, N. G. Almarza, M. A. González, and F. J. Bermejo, Phys. Rev. E **57**, 4486 (1998).

[72] V. Krakoviack, J.-P. Hansen, and A. A. Louis, Phys. Rev. E **67**, 041801 (2003).

[73] A. Pelissetto and J.-P. Hansen, J. Chem. Phys. **122**, 134904 (2005).